2D piecewise affine models approximate real continuous dynamics up to invariant sets

Madalena Chaves, Jean-Luc Gouzé

2D piecewise affine models approximate real continuous dynamics up to invariant sets ⋆

Madalena Chaves * **Jean-Luc Gouzé** *

* *Inria, Project-team BIOCORE,*
2004 Route des Lucioles, BP 93, 06902 Sophia Antipolis, France
{*madalena.chaves,jean-luc.gouze*}*@inria.fr*

Abstract: Piecewise affine models often provide a good approximation to describe continuous systems, but may involve a high degree of simplification. To compare solutions of the continuous and piecewise affine models, it is important to quantify the differences between solutions in each region of the state space. As an approach, we will use enveloping "bands" to characterize continuous activation or inhibition functions, and then describe the differences between continuous and piecewise affine solutions in terms of the width δ of these bands. As a case study, we will consider the negative feedback loop, a classical motif in two dimensions which results in oscillating behaviour. For this example, it is shown that the two types of models may differ only on a compact invariant set (the interior of a limit cycle), whose diameter is a function of the band width δ.

Keywords: Piecewise affine models, ordinary differential equations, hybrid systems, approximation, invariant sets.

1. INTRODUCTION

Piecewise affine models consist on systems of differential equations whose vector fields are based on a combination (sums of products) of step functions and are amenable to the use of theoretical analysis tools. This modeling framework has been introduced by L. Glass and co-authors (Glass and Kauffman, 1973), to describe and represent the dynamics of biological (e.g., genetic) regulatory networks. They have developed several qualitative results, including a classification of systems according the existence of oscillatory behavior (Glass and Pasternak, 1978). Applications to genetic networks include the study of the carbon stress response in *Escherichia coli* (Ropers et al., 2006) and the segment polarity genes family in *Drosophila Melanogaster* (Chaves et al., 2006).

To understand the connection between solutions of a piecewise affine model and those of a continuous system, several approaches have been suggested, based on a continuous approximation of the step function and then studying the limit (de Jong, 2002; Plahte et al., 1994).

A more general formulation is suggested here (see Section 2.2), where the continuous system is composed of activation and inhibition functions; these are represented by two constants (zero and one) separated by a band (of width δ) enveloping a threshold region in the phase space, which allows a continuous transition from zero to one (no particular mathematical expression is assumed for this transition region) or from one to zero. Similar approaches have been proposed before in Chaves et al. (2008); Plahte et al. (1994).

To study and apply this formalism, we will focus on a two-dimensional negative feedback loop (see Section 3), which represents a frequent motif in complex regulatory networks (Thomas and d'Ari, 1990), in particular it is at the core of the *E. coli* carbon starvation model developed in Ropers et al. (2006). Our objective is to characterize the regions of the state space where the trajectories of the continuous and piecewise affine systems have the same or similar qualitative dynamics, as well as those regions where their dynamics diverges.

Two main results from our analysis are to be pointed out (see Sections 4 and 5): (i) first, the region where qualitative differences occur between the behavior of continuous and piecewise affine models can be quantified in terms of the band width δ; (ii) second, trajectories of both systems converge towards this region; while the continuous system may indeed exhibit some dynamics not modeled by the piecewise affine systems, these are confined to a compact invariant set $\bar{\mathcal{C}}$, which can be quantified and has a diameter which is a function of δ and tends to zero with δ.

Our tools are the construction of two outer and inner piecewise linear systems that will enclose the smooth system. We study the dynamical behaviour of these two systems, and obtain bounds for the smooth one, for a given width δ of the band. Unlike other works (Plahte et al., 1994), our approach (similar to Chaves et al. (2008)) is not a limit approach, and gives results for a fixed δ. A related idea is found in Shu and Sanfelice (2014), where the work is oriented toward hybrid systems and hysteresis.

⋆ This work was supported in part by the projects GeMCo (ANR 2010 BLANC020101), RESET (Bioinformatique, ANR-11-BINF-0005), and by the LABEX SIGNALIFE (ANR-11-LABX-0028-01).

2. CONTINUOUS AND PIECEWISE AFFINE MODELS

Protein and gene interactions in genetic networks are often well described by sigmoid-like functions (Yagil and Yagil, 1971), where abrupt changes in transcription (or synthesis rates) are observed once a given transcription factor has reached a certain threshold concentration. Continuous models of large genetic networks can be very complex: while numerical simulations provide good results, theoretical analysis is rarely possible without simplifying the mathematical system. A possible approach is to consider interactions with only two states On or Off (Thomas, 1973; Glass and Kauffman, 1973), thus approximating sigmoid-like functions by piecewise constant *step* functions.

2.1 PWA systems

This approximation leads to the formulation of *piecewise affine (PWA) differential equations* models (de Jong, 2002) and, in particular, it has led to the development of a qualitative method for analysis of genetic networks (de Jong et al., 2003). We very briefly review the PWA formalism and notation (for more details see Casey et al. (2006). Define the increasing (or activation) step function as:

$$s^+(x,\theta) = \begin{cases} 0, & x < \theta \\ 1, & x > \theta \end{cases} \tag{1}$$

and the decreasing (or inhibition) step function as $s^-(x,\theta) = 1 - s^+(x,\theta)$.

The equations for variable $x_i \in [0,+\infty)$ $(i = 1,\ldots,n)$ is:

$$\dot{x_i} = f_i(x;\theta_{j_1,i},\ldots,\theta_{j_{p_n},i}) - \gamma_i x_i$$

where functions f_i represent the dependence of the rate of synthesis of a protein encoded by gene i on the concentrations x_j of the other proteins in the cell, and θ_j are thresholds, with:

$$f_i(x) = \sum_{l\in I} \kappa_{il} b_{il}(x), \tag{2}$$

where $\kappa_{il} > 0$ is a rate parameter, $b_{il} : \mathbb{R}^n_{\geq 0} \to \{0,1\}$ is a Boolean-valued regulation function, and I is an index set. The regulation functions b_{il} summarize the incoming interactions at node i, and are typically written as combinations (sums of products) of step functions with thresholds θ_j. The γ_i are constant degradation rates.

The thresholds partition the state space into several rectangular regions, or *regular domains*. Inside each regular domain, D_J, the vector field is linear and decoupled, and solutions of the system can be explicitly computed. As t tends to infinity, the solution would tend to the point $\phi_{ij} = \kappa_{ij}/\gamma_i$, with $\phi = (\phi_{1j_1},\ldots,\phi_{nj_n})$ called the *focal point* of domain D_J. However, as soon as the trajectories hit the boundary of D_J, the vector field switches. The full trajectory is thus a concatenation of the solutions in each successive regular domain. Note that the vector field is discontinuous and not defined at the threshold values, $x_i = \theta_{i,j}$ for all $i = 1,\ldots,n$, $j = 1,\ldots,p_i$. However, solutions of the system (2) "across" or "along" a threshold can still be defined in the sense of Filippov, as the solutions of differential inclusions (see Casey et al. (2006) for more details). We do not need these notions in the paper.

2.2 A general formulation for continuous systems

Now we describe the continuous systems associated to these PWA systems. Two widely used continuous models for regulatory networks substitute the step functions either by Hill functions (de Jong, 2002) or *logoids* (saturated linear functions) (Plahte et al., 1994).

We now propose a more generally formulated function which coincides with the step function outside a (small) interval around the threshold value, and may be any differentiable function in the transition interval (see also Chaves et al. (2008)). Given positive constants θ, κ, and δ with

A1. $\delta \in (0,\theta)$ such that $\kappa/\gamma - (\theta \pm \delta) > 0$;

and a transition function $\mu_{trans} : [\theta-\delta,\theta+\delta] \to [0,1]$ with the following properties:

A2. $\mu_{trans}(\theta-\delta) = 0$, $\mu_{trans}(\theta+\delta) = 1$, and $\mu_{trans}(x) \in (0,1)$ for all $x \in (\theta-\delta,\theta+\delta)$;
A3. μ_{trans} is continuously differentiable;

define:

$$\mu^+(x,\theta;\delta) = \begin{cases} 0, & 0 \leq x \leq \theta-\delta \\ \mu_{trans}(x), & \theta-\delta \leq x \leq \theta+\delta \\ 1, & \theta+\delta \leq x. \end{cases} \tag{3}$$

Note that (3) contains both the Hill [1] and logoid formulation (with $\mu_{trans}(x) = \frac{1}{2\delta}(x-(\theta-\delta))$), but in general the transition function can be very freely chosen, for instance, it doesn't have to be monotonic. A similar definition holds for inhibition functions $\mu^-(x,\theta;\delta) = 1 - \mu^+(x,\theta;\delta)$. For the comparison between PWA and continuous systems, we will focus on the case of *small* δ, and will not deal with the case $\delta \to 0$. The form of the model (2) remains unchanged, replace only the step functions by the corresponding, more general, functions of the form (3).

3. THE (SHIFTED) 2D NEGATIVE LOOP

As an example, consider the two-node network $\{x \to y, y \dashv x\}$ which represents a frequent motif in complex regulatory networks. It is one of the most classical motifs in gene networks, together with the bistable switch (Thomas and d'Ari, 1990). For instance, the model of the *E. coli* nutritional stress response developed in Ropers et al. (2006) can be reduced to a two-dimensional negative feedback loop, in the presence of glucose (as shown in Grognard et al. (2007)).

Let κ_1, κ_2, γ_1, and γ_2 be positive constants, and θ_1, and θ_2 the thresholds associated with each interaction. Assume that $\kappa_i/\gamma_i - \theta_i > 0$. Using step functions, the 2-dimensional negative feedback loop is modeled as:

$$\Sigma : \quad \begin{aligned} \dot{x} &= \kappa_1 s^-(y,\theta_2) - \gamma_1 x \\ \dot{y} &= \kappa_2 s^+(x,\theta_1) - \gamma_2 y, \end{aligned} \tag{4}$$

[1] In fact, it is not exactly the Hill function, but a function taking the values zero and one outside the central band where it is a Hill formulation chosen to obtain continuity.

It has been shown that system (4) converges towards the point (θ_1, θ_2) (Glass and Pasternak, 1978). The corresponding smooth system is:

$$\Sigma_\delta : \quad \begin{aligned} \dot{x} &= \kappa_1 \mu^-(y, \theta_2; \delta) - \gamma_1 x \\ \dot{y} &= \kappa_2 \mu^+(x, \theta_1; \delta) - \gamma_2 y \end{aligned} \tag{5}$$

To analyze (5), we first study a limiting case, obtained by choosing functions μ^- and μ^+ which provide upper and lower bounds for trajectories of (5). Systems (5) and (4) have exactly the same vector fields outside the bands enveloping the threshold values, that is outside $[\theta_1 - \delta, \theta_1 + \delta] \times [0, \infty)$ and $[0, \infty) \times [\theta_2 - \delta, \theta_2 + \delta]$. So the qualitative dynamics of the continuous and PWA systems are the same outside these regions. Within these regions, trajectories of (5) deviate from trajectories of (4). Maximal deviation (the upper bound) corresponds to a system where the vector field (5) switches only at the "last possible value": for instance, in the left half of the plane $(x < \theta_1 - \delta)$, let $\mu^+(y, \theta_y) = 0$ for all $y > \theta_2 - \delta$, while in the right half of the plane $(x > \theta_1 + \delta)$, let $\mu^+(y, \theta_y) = 0$ for all $y > \theta_2 + \delta)$. This gives rise to an outer system of the form (2), which generates a *shifted negative feedback loop*, defined for all $(x, y) \notin [\theta_1^-, \theta_1^+] \times [\theta_2^-, \theta_2^+]$:

$$\begin{aligned} \dot{x} &= \kappa_1 \left[s^-(y, \theta_2^+) s^+(x, \theta_1^+) + s^-(y, \theta_2^-) s^-(x, \theta_1^+) \right] - \gamma_1 x \\ \dot{y} &= \kappa_2 \left[s^+(x, \theta_1^+) s^-(y, \theta_2^+) + s^+(x, \theta_1^-) s^+(y, \theta_2^+) \right] - \gamma_2 y \end{aligned} \tag{6}$$

(where $\theta_i^- = \theta_i - \delta$ and $\theta_i^+ = \theta_i + \delta$) whose trajectories "enclose" the trajectories of any system of the form (5) (see Fig. 1). The phase plane is thus partitioned into four orthants separated by bands of width 2δ and a small square region in the middle. The four shifted orthants are

$$\begin{aligned} Q_{01} &= \{(x, y) \in \mathbb{R}^2 : \ x \in [0, \theta_1 - \delta), \ y \in (\theta_2 - \delta, \infty)\} \\ Q_{00} &= \{(x, y) \in \mathbb{R}^2 : \ x \in [0, \theta_1 + \delta), \ y \in [0, \theta_2 - \delta)\} \\ Q_{10} &= \{(x, y) \in \mathbb{R}^2 : \ x \in (\theta_1 + \delta, \infty), \ y \in [0, \theta_2 + \delta)\} \\ Q_{11} &= \{(x, y) \in \mathbb{R}^2 : \ x \in (\theta_1 - \delta, \infty), \ y \in (\theta_2 + \delta, \infty)\}. \end{aligned}$$

The fact that the transition thresholds are not aligned with respect to left/right or up/bottom half planes, implies that system (6) is not of the form studied in Glass and Pasternak (1978), even though it is still a negative feedback loop. In fact, we will next show that system (6) converges to a limit cycle around the middle region $[\theta_1 - \delta, \theta_1 + \delta] \times [\theta_2 - \delta, \theta_2 + \delta]$. In a similar way, we define a

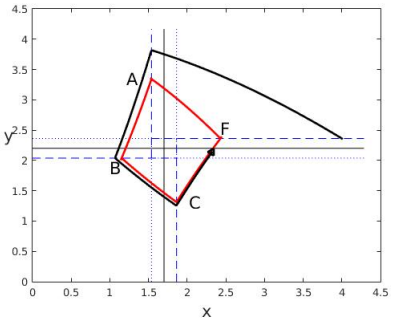

Fig. 1. The limit cycle (red) and a trajectory (black) of system (6). The parameters are: $\kappa_1 = 3$, $\kappa_2 = 5$, $\theta_1 = 1.7$, $\theta_2 = 2.2$, $\gamma_1 = 0.7$, $\gamma_2 = 1.2$, and $\delta = 0.16$.

lower bound or inner PWA approximation, which switches at the "first possible value" and will be shown to converge toward (θ_1, θ_2).

4. EXISTENCE OF A LIMIT CYCLE

Now, we will compute the first return map for (6), and show that it has a unique fixed point (see Fig. 1). In addition, we will show that this fixed point is outside the middle region, and that trajectories starting outside converge towards this point. To simplify notation, define

$$A_i = \frac{\kappa_i}{\gamma_i}, \theta_i^+ = \theta_i + \delta, \theta_i^- = \theta_i - \delta \ \ (i = 1, 2), \text{ and } \gamma = \frac{\gamma_1}{\gamma_2}.$$

For technical reasons (which will become clear in Lemma 4.4 below), assume that: $\left(\frac{\theta_2^-}{A_2}\right)^\gamma < \theta_1^-$. Morever, assumptions A1 and A2 hold for every index i. In the following results, it will be assumed that trajectories of (6) are evolving in $[0, A_1] \times [0, A_2]$, since this is an invariant set for the system. Define the functions (invertible in their domains):

$$h_1(r) = \frac{\theta_1^- r - A_1}{\theta_1^+ - A_1}, \quad h_2(r) = \left(\frac{\theta_2^+ - A_2}{\theta_2^- \frac{1}{r^{1/\gamma}} - A_2} \right)^\gamma,$$

with domains $h_1 : [0, A_1/\theta_1^-] \to [0, A_1/(A_1 - \theta_1^+)]$ and $h_2 : ((\theta_2^-/A_2)^\gamma, \infty) \to ((A_2 - \theta_2^+)/A_2, \infty)$. Some basic properties of these functions are next summarized:

Lemma 4.1. Assume $\theta_i^+ < A_i$ $(i = 1, 2)$ and $(\theta_2^-/A_2)^\gamma < \theta_1^-$. The functions h_1 and h_2 satisfy:

$$(a) \ \ \frac{dh_1}{dr} = \frac{\theta_1^-}{\theta_1^+ - A_1} < 0, \quad h_1(0) = \frac{A_1}{A_1 - \theta_1^+}, \quad h_1\left(\frac{A_1}{\theta_1^-}\right) = 0;$$

$$(b) \ \ \frac{dh_2}{dr} = -\theta_2^- h_2(r) \frac{1}{r} \frac{1}{A_2 r^{1/\gamma} - \theta_2^-} < 0,$$
$$\lim_{r \to (\theta_2^-/A_2)^\gamma} h_2(r) = \infty, \quad \lim_{r \to \infty} h_2(r) = \left(\frac{A_2 - \theta_2^+}{A_2} \right)^\gamma;$$

$$(c) \ \ h_1(r) > r \ \text{ if and only if } \ r \in \left(0, \frac{A_1}{A_1 - (\theta_1^+ - \theta_1^-)}\right);$$

$$(d) \ \ \left| \frac{dh_1 \circ h_2}{dr}(s) \right| > \left| \frac{dh_2 \circ h_1}{dr}(s) \right|, \ \forall \ s \in L = \left(\left(\frac{\theta_2^-}{A_2} \right)^\gamma, 1 \right).$$

■

To compute the Poincaré map for this system, we will follow the trajectory of a point starting on the segment $Y_0 = \theta_2^+$ with $\theta_1^+ < X_0 < A_1$:
$(X_0, \theta_2^+) \rightsquigarrow (\theta_1^-, Y_A) \rightsquigarrow (X_B, \theta_2^-) \rightsquigarrow (\theta_1^+, Y_C) \rightsquigarrow (X_F, \theta_2^+)$.

Lemma 4.2. The Poincaré map of system (6) is given by $f : [0, A_1] \to [0, A_1]$:

$$f(x) = \theta_1^- \ h_1^{-1} \circ h_2 \circ h_1 \circ h_2^{-1} \left(\frac{x}{\theta_1^-} \right). \tag{7}$$

Proof: In general, solving the linear equations $\dot{x} = \gamma_1(\phi_1 - x)$ and $\dot{y} = \gamma_2(\phi_2 - x)$ in each quadrant, the trajectories from a point $P_a = (x_a, y_a)$ to a point $P_b = (x_b, y_b)$, satisfy:

$$\frac{x_b - \phi_1}{x_a - \phi_1} = e^{-\gamma_1 (t_b - t_a)}, \qquad \frac{y_b - \phi_2}{y_a - \phi_2} = e^{-\gamma_2 (t_b - t_a)}, \tag{8}$$

where $\phi_i \in \{0, A_i\}$ denotes the appropriate focal point. Thus,

$$\frac{x_b-\phi_1}{x_a-\phi_1}=\left(\frac{y_b-\phi_2}{y_a-\phi_2}\right)^{\gamma}.$$

The expression of the Poincaré map follows after some computations. ∎

The existence of a fixed point of the Poincaré map can be deduced from the following Lemma.

Lemma 4.3. There is a unique solution r^* of $h_1\circ h_2(r^*)=h_2\circ h_1(r^*)$ in the interval $L=((\theta_2^-/A_2)^\gamma,1)$.

Proof: To prove this result, let $\varepsilon>0$ be a small number and choose a real number z such that:

$$z=\left(\theta_2^-/A_2\right)^\gamma+\varepsilon<1,\quad h_2(z)=A_1/\theta_1^-$$

(this choice is possible, by Lemma 4.1). We will show that:

(a) $h_1\circ h_2(z)<h_2\circ h_1(z)$;
(b) $h_1\circ h_2(1)>h_2\circ h_1(1)$;
(c) $\left|\frac{dh_1\circ h_2}{dr}(s)\right|>\left|\frac{dh_2\circ h_1}{dr}(s)\right|$, for all $s\in L$.

First, observe that h_1 and h_2 are both strictly decreasing (Lemma 4.1). Next, note that $h_1\circ h_2(z)=h_1(A_1/\theta_1^-)=0$ and that, for any z, $h_2\circ h_1(z)>\frac{A_2-\theta_2^+}{A_2}$ so, for some appropriately small $\varepsilon>0$, part (a) is true. It is easy to check that (b) is also true:

$$h_1\circ h_2(1)=h_1\left(\left(\frac{\theta_2^+-A_2}{\theta_2^--A_2}\right)^\gamma\right)>\frac{\theta_1^--A_1}{\theta_1^+-A_1}>1$$

$$h_2\circ h_1(1)=h_2\left(\frac{\theta_1^--A_1}{\theta_1^+-A_1}\right)<\left(\frac{\theta_2^+-A_2}{\theta_2^--A_2}\right)^\gamma<1.$$

Finally, statement (c) follows directly from Lemma 4.1(d). From (a) and (b), we conclude that $h_1\circ h_2$ and $h_2\circ h_1$ intersect at least once, in the interval L: as a composition of two decreasing functions, both $h_1\circ h_2$ and $h_2\circ h_1$ are strictly increasing; from (c), $h_1\circ h_2$ increases strictly faster than $h_2\circ h_1$; and from (a) $h_1\circ h_2$ starts at a lower value than $h_2\circ h_1$, so that the functions can only intersect once, as claimed. ∎

Lemma 4.4. The Poincaré map (7) has a unique fixed point, X^*, and it is stable.

Proof: First, we will show the map (7) has a unique fixed point, and then that $|df/dx|<1$, to show that it is stable.

$$h_1\left(\frac{x_0}{\theta_1^-}\right)=h_1\circ h_2\left(\frac{x_B}{\theta_1^-}\right)\quad\text{and}\quad h_1\left(\frac{x_F}{\theta_1^-}\right)=h_2\circ h_1\left(\frac{x_B}{\theta_1^-}\right)$$

Note that x_0/θ_1^- is in the domain of h_1 (since $x_0\in[0,A_1]$); and also $x_B\in(0,\theta_1^-)$ (see also Fig. 1). Finding a fixed point of the Poincaré map is thus equivalent to finding x_B that satisfies $x_0=x_F$, that is:

$$h_1\circ h_2\left(\frac{x_B}{\theta_1^-}\right)=h_2\circ h_1\left(\frac{x_B}{\theta_1^-}\right).$$

Since $x_B<\theta_1^-$ and by definition of the domain of h_2, any fixed point of f must be in the interval $\left(\left(\theta_2^-/A_2\right)^\gamma,\theta_1^-\right)$. Then, by Lemma 4.3, there is a unique fixed point of f and it is of the form $X^*=r^*\theta_1^-$. To check stability, the chain rule and Lemma 4.1 show that $|df/dx(X^*)|<1$.

The existence of a unique, stable, fixed point for the Poincaré map implies the next result.

Theorem 1. For each $0<\delta<\min\{\theta_1,\theta_2\}$, the system (6) admits a limit cycle, $\mathcal{C}_\delta$, passing through the point $(X^*,\theta_2+\delta)$, where $X^*=X^*(\delta)$ is the unique fixed point of the Poincaré map f. Trajectories starting outside the region enclosed by $\mathcal{C}_\delta$ converge towards it. As $\delta\to0$,

$$\lim_{\delta\to0}X^*(\delta)=\theta_1,\quad\text{and}\quad\lim_{\delta\to0}\mathcal{C}_\delta\to\{(\theta_1,\theta_2)\}.$$

Proof: To prove the results as $\delta\to0$, observe that the interval where the fixed point is located can be reduced further to:

$$(z_1,z_2):=\left(\left(\frac{\theta_2^-}{\theta_2^+}\right)^\nu,\left(\frac{\theta_2^-}{\theta_2^+}\right)^\gamma\right),$$

where $\nu>\gamma$ can be chosen such that (using Lemma 4.1),

$$z_1=\left(\theta_2^-/\theta_2^+\right)^\nu\quad\text{and}\quad h_2(z_1)=A_1/\theta_1^-.$$

This implies $h_1\circ h_2(z_1)=0$, so that $h_1\circ h_2(z_1)<(A_2-\theta_2^+)/A_2<h_2\circ h_1(z_1)$, as in the proof of Lemma 4.3, part(a). Next, one has $h_2(z_2)=1$ and $h_1(1)=(A_1-\theta_1^-)/(A_1-\theta_1^+)>1$, that is $h_1\circ h_2(z_1)>1$; while $h_1(z_2)>1$ implies $h_2\circ h_1(z_2)<1$. We then have $h_2\circ h_1(z_2)<h_1\circ h_2(z_2)$. Therefore, as in the argument of Lemma 4.3, we conclude that the functions $h_2\circ h_1$ and $h_1\circ h_2$ intersect exactly once in the interval (z_1,z_2), which also implies $r^*\in(z_1,z_2)$. Since $\theta_2^\pm=\theta_2\pm\delta$, the interval for r^* tends to $\{1\}$, as $\delta\to0$. Hence, the point $(X^*,\theta_2+\delta)$ (and the curve $\mathcal{C}_\delta$) tend to (θ_1,θ_2). ∎

Similarly, the study of the inner PWA approximation can be done, and it is easy to see that it has an attractor at (θ_1,θ_2).

We are now interested in the results for a finite *fixed* δ.

5. CONVERGENCE TO A COMPACT SET

The four segments constituting the limit cycle $\mathcal{C}_\delta$ (see Fig. 1) can be parametrized as:

$$\mathcal{C}=\{(g_q(z),z):\ z\in I_q,\quad q\in\{01,00,10,11\}\}$$

where q denotes one of the four orthants defined above (Q_{01}, Q_{00}, Q_{10}, or Q_{11}), and the functions g_q are defined using expressions (8), as follows. Let x_B denote the intersection of $\mathcal{C}_\delta$ with the segment (θ_1,A_1) and $y=\theta_2^+$, and y_A (resp., y_C) denote the intersection of $\mathcal{C}_\delta$ with the segment (θ_2,A_2) and $x=\theta_1^-$ (resp., $(0,\theta_2)$ and $x=\theta_1^+$).

$$I_{01}=[\theta_2^-,y_A],\quad g_{01}(z)=\theta_1^-\left(\frac{z}{y_A}\right)^\gamma$$

$$I_{00}=[y_C,\theta_2^-],\quad g_{00}(z)=A_1-(A_1-x_B)\left(\frac{z}{\theta_2^-}\right)^\gamma$$

$$I_{10}=[y_C,\theta_2^+],\quad g_{10}(z)=A_1-(A_1-\theta_1^+)\left(\frac{A_2-z}{A_2-y_C}\right)^\gamma$$

$$I_{11}=[\theta_2^+,y_A],\quad g_{11}(z)=x_B\left(\frac{A_2-z}{A_2-\theta_2^+}\right)^\gamma$$

Let $\bar{\mathcal{C}}$ denote the compact set enclosed by the closed curved $\mathcal{C}_\delta$. To show that trajectories of (5) converge towards this

compact set, we will use a function that measures the distance to the set $\bar{\mathcal{C}}$, from each point in the plane. By definition, such a function will be zero at any point in the set $\bar{\mathcal{C}}$. At each point $(x,y) \in \mathbb{R}^2_{\geq 0}$ define function $V(x,y)$:

$$\begin{cases} \min\limits_{z\in I_{01}} \left\{ |y-z| + \frac{1}{\gamma}\frac{\theta_2^-}{\theta_1^-}\,|x-g_{01}(z)| \right\}, & \text{if } (x,y)\in Q_{01}\setminus\bar{\mathcal{C}} \\ \min\limits_{z\in I_{00}} \left\{ \frac{A_1-\theta_1^+}{\theta_1^-}\{|y-z| + \frac{1}{\gamma}\frac{\theta_2^-}{\theta_1^-}\,|x-g_{00}(z)| \right\}, & \text{if } (x,y)\in Q_{00}\setminus\bar{\mathcal{C}} \\ \min\limits_{z\in I_{10}} \left\{ \frac{A_1-\theta_1^+}{\theta_1^-}\,|y-z| + \frac{1}{\gamma}\frac{A_2-\theta_2^+}{\theta_1^-}\,|x-g_{10}(z)| \right\}, & \text{if } (x,y)\in Q_{10}\setminus\bar{\mathcal{C}} \\ \min\limits_{z\in I_{11}} \left\{ |y-z| + \frac{1}{\gamma}\frac{A_2-\theta_2^+}{\theta_1^-}\,|x-g_{11}(z)| \right\}, & \text{if } (x,y)\in Q_{11}\setminus\bar{\mathcal{C}} \\ 0, & \text{if } (x,y)\in\bar{\mathcal{C}}\ . \end{cases} \tag{9}$$

We will next show that V is a "flat" Lyapunov function for system (5). It is clear that $V(x,y)$ is zero if and only if $(x,y) \in \bar{\mathcal{C}}$. Indeed, since $(g_q(z),z)$ parametrizes the boundary of $\bar{\mathcal{C}}$ in orthant Q_q, $V(x,y)$ is zero whenever (x,y) belongs to the boundary of $\bar{\mathcal{C}}$. Otherwise, V is strictly positive, as the sum of positive values. It is not difficult to show that V is continuous. A more detailed characterization of V, including explicit expressions, can be obtained based on minimizing the function W with respect to z:

$$W(r,s,z) = S\,|s-z| + R\,|r-g(z)|\,.$$

where $S=1$ and $R = \frac{1}{\gamma}\frac{\theta_2^-}{\theta_1^-}$ in Q_{01}. Proposition 1 below characterizes the decrease of V along trajectories evolving in Q_{01}. Let V^{01} denote the function V in the orthant Q_{01}. The same arguments will apply to the other orthants, under appropriate changes of variables. For this reason, in this Section, a "general" set of coordinates will be adopted, (r,s), with:

$$\gamma = \frac{\gamma_r}{\gamma_s}, \quad \hat{\theta}_{r,s} = \theta^-_{r,s}, \quad \frac{R}{S} = \frac{1}{\gamma}\frac{\hat{\theta}_s}{\hat{\theta}_r}, \quad s_\alpha = y_A, \quad r_\beta = g(\hat{\theta}_s)$$

and

$$g(s) = \hat{\theta}_r\,(s/s_\alpha)^\gamma \quad \text{and} \quad g^{-1}(r) = s_\alpha\left(r/\hat{\theta}_r\right)^{\frac{1}{\gamma}}\ .$$

Recall also that the boundary of $\bar{\mathcal{C}}$ in Q_{01} is defined by $s = g^{-1}(r)$, so that we are interested in pairs $(r,s) \in Q_{01}\setminus\bar{\mathcal{C}}$, that is $s > \max\{\hat{\theta}_s, g^{-1}(r)\}$.

Proposition 1. Given any $\delta > 0$, there exists a constant $c = c(\gamma_r,\gamma_s)$ such that:

$$\nabla V^{01}\,f(r,s;\delta) < -cV^{01}(r,s), \quad \forall\ (r,s)\in Q_{01}\setminus\bar{\mathcal{C}}.$$

Proof: Fix any $\delta > 0$. Recall the definition of Q_{01} (9), and note that

$$f_r(r,s;\delta) \leq \mu_1^-(s,\theta_s;\delta) - \gamma_r r \quad \text{and} \quad f_s(r,s;\delta) = -\gamma_s s$$

that is, coordinate s is strictly decreasing on Q_{01}, while coordinate r is decreasing as long as $s \geq \theta_s + \delta$, but may be increasing for $\theta_s - \delta \leq s < \theta_s + \delta$ (depending on the function μ_1^-).

It can be shown that $V^{01} = V_i$ depending on which of the four regions of the Q_{01} orthant (r,s) belongs to. We will show that $\nabla V^i\,f(r,s;\delta) < -cV^i(r,s)$ holds for each $i=1,\ldots,4$, in its corresponding region. Assume first that $s > s_\alpha$ and consider $V_1(r,s) = R(\hat{\theta}_r - r) + S(s-s_\alpha)$:

$$\begin{aligned} \nabla V_1\,f(r,s;\delta) &= -R(\mu_1^-(r,\theta_r;\delta) - \gamma_r r) + S(-\gamma_s s) \\ &= \gamma_s\left[-\frac{1}{\gamma_s}R\mu_1^-(r,\theta_r;\delta) + \gamma R r - \gamma R\hat{\theta}_r - Ss + Ss_\alpha\right] \\ &\quad +\gamma_s(\gamma R\hat{\theta}_r - Ss_\alpha) \\ &< -\gamma_s\min\{1,\gamma\}\left[R(\hat{\theta}_r - r) + S(s-s_\alpha)\right] \\ &< -\gamma_s\min\{1,\gamma\}V_1(r,s) \end{aligned}$$

where the second equality was obtained by first putting γ_s in evidence, and then adding and subtracting the quantity $\gamma R\hat{\theta}_r - Ss_\alpha$. The inequality in the third line follows by using $-\frac{1}{\gamma_s}R\mu_1^-(r,\theta_r;\delta) \leq 0$ and observing that

$$\gamma R\hat{\theta}_r - Ss_\alpha = S\hat{\theta}_s - Ss_\alpha < 0.$$

The cases for the other V_i are treated similarly. ∎

As a corollary, we conclude that V satisfies a similar estimate for all $(x,y) \in \mathbb{R}^2_{\geq 0}$.

Proposition 2. There exist a constant $c = c(\gamma_1,\gamma_2)$ such that

$$\nabla V\,f(x,y;\delta) < -cV(x,y), \quad \forall\ (x,y)\in\mathbb{R}^2_{\geq 0}\setminus\bar{\mathcal{C}}$$

and $\nabla V\,f(x,y;\delta) = 0$, for all $(x,y)\in\bar{\mathcal{C}}$.

Proof: It is enough to apply Proposition 1 to each orthant using appropriate variables (these correspond to a clockwise rotation, until the desired orthant coincides with Q_{01}). We cannot detail here.

The convergence of the trajectories of system (5) can now be shown.

Theorem 2. Trajectories of (5) converge towards the compact set enclosed by the limit cycle $\mathcal{C}$.

Proof: First, note that, for any $\xi \in \mathbb{R}^2_{\geq 0}$

$$\text{dist}(\xi,\bar{\mathcal{C}}) \leq \max\left\{1, \frac{\theta_1^-}{A_1-\theta_1^+}, \gamma\frac{\theta_1^-}{\theta_2^-}, \gamma\frac{\theta_1^-}{A_2-\theta_2^+}\right\}V(\xi)\ = c_3V(\xi).$$

Now consider a solution of (5), $(x(t),y(t))$ and let $\psi(t) = V(x(t),y(t))$. Apply Proposition 2 to conclude that

$$\frac{d\psi}{dt} = \nabla V\ f(x,y;\delta) < -c\psi(t),$$

for some positive constant c. Integration yields $\psi(t) \leq \psi(0)\,e^{-ct}$, implying that the distance between $(x(t),y(t))$ and $\bar{\mathcal{C}}$ tends to zero as time tends to infinity. ∎

6. SIZE OF THE LIMIT CYCLE

It is interesting to explore the links between the band width δ and the size of the limit cycle. First, in the proof of Theorem 1, it is easy to obtain (from the estimate of X^*) that a rough estimate of the size of one radius of the limit cycle along the axis $y = \theta_2 - \delta$ is

$$R(\delta) = \theta_1 - (\theta_1^-)\left(\frac{\theta_2^-}{\theta_2^+}\right)^\gamma \tag{10}$$

Of course, $R(0) = 0$ and $R(\theta_1) = \theta_1$, and function R is increasing. The first term of the Taylor expansion around $\delta = 0$ is $(2\theta_1\gamma/\theta_2 + 1)$. If we choose (to simplify) $\theta_1\gamma/\theta_2 = 1, \gamma = \theta_1/\theta_2 = 1$, then function R/θ_1 is concave between 0 and 1, and admits a maximum for $\delta = 1$, with an initial slope of 3.

We checked numerically, for arbitrary values of the parameters, these findings (cf. Fig2). It is shown on the figure that the estimate is close to the real value of the radius of the limit cycle, except around zero, and also the concave form of the curve in function of δ.

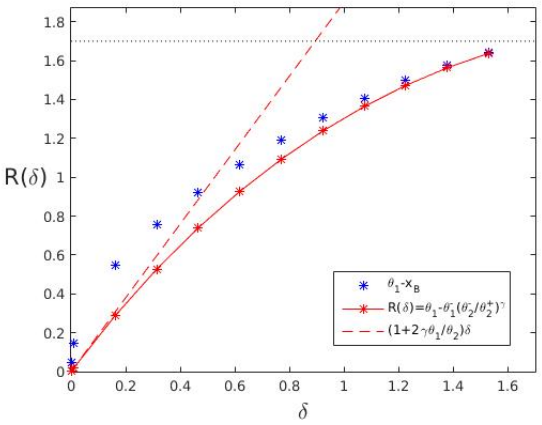

Fig. 2. Size of the limit cycle w.r.t. band width δ: blue: numerical results; red curve: estimates with (10); dashed red: first order approximation.

7. EXTENSION TO N-DIMENSIONAL LOOPS

These results can be extended for higher dimensional negative loops. Assuming that the system is of a simple form $\{x \to z, z \to y, y \dashv x\}$, with a single threshold associated to each variable, a similar idea can be applied, by considering functions $\mu^{\pm}$ instead of step functions. In this case, one question is whether trajectories of the general system will still converge towards a compact set. For instance (under an appropriate parameter choice) the 3D negative loop is known to exhibit a limit cycle (Farcot and Gouzé, 2009), so it is expected that trajectories of the general system using functions $\mu^{\pm}$ will stay in an "annular" region enclosing the nominal limit cycle (see Poignard et al. (2016)).

8. CONCLUSIONS

This work shows how a continuous system can be bounded by two piecewise affine systems, which generate outer and inner bounds for its trajectories. Application to a 2-dimensional negative loop shows that the qualitative behavior of the continuous and PWA systems are quite similar except on a compact invariant set. Trajectories of both systems will converge towards this set (Theorems 1 and 2). Inside this compact set, the behavior of the continuous system depends on the transition part of the continuous system, and cannot be predicted by the PWA systems. However, the diameter of this set decreases with the width δ of the transition interval, and shrinks to a single point in the phase space when $\delta \to 0$.

In practice, many genetic and signaling interactions have switch-like properties which translate to narrow transition regions, and we think that this approach may give new tools to study continuous systems with the help of their "enveloping" PWA systems. The resulting behaviour are similar, up to some invariant sets, where anything can happen; but their size is small when band width δ is small.

REFERENCES

Casey, R., de Jong, H., and Gouzé, J. (2006). Piecewise-linear models of genetic regulatory networks: equilibria and their stability. *J. Math. Biol.*, 52, 27–56.

Chaves, M., Eissing, T., and Allgöwer, F. (2008). Bistable biological systems: a characterization through local compact input-to-state stability. *IEEE Trans. Automat. Control*, 53, 87–100.

Chaves, M., Sontag, E., and Albert, R. (2006). Methods of robustness analysis for boolean models of gene control networks. *IEE Proc. Syst. Biol.*, 153, 154–167.

de Jong, H. (2002). Modeling and simulation of genetic regulatory systems: A literature review. *J. Comput. Biol.*, 9(1), 67–103.

de Jong, H., Geiselmann, J., Hernandez, C., and Page, M. (2003). Genetic network analyzer : Qualitative simulation of genetic regulatory networks. *Bioinformatics*, 19(3), 336–344.

Farcot, E. and Gouzé, J. (2009). Periodic solutions of piecewise affine gene network models with non uniform decay rates: The case of a negative feedback loop. *Acta Biotheoretica*, 57(4), 429–455.

Glass, L. and Kauffman, S. (1973). The logical analysis of continuous, nonlinear biochemical control networks. *J. Theor. Biol.*, 39, 103–129.

Glass, L. and Pasternak, J. (1978). Stable oscillations in mathematical models of biological control systems. *J. Math. Biol.*, 6, 207–223.

Grognard, F., Gouzé, J.L., and de Jong, H. (2007). Piecewise-linear models of genetic regulatory networks: theory and example. In I. Queinnec and al. (eds.), *Biology and control theory: current challenges*, LNCIS 357, 137–159. Springer-Verlag.

Plahte, E., Mestl, T., and Omholt, S. (1994). Global analysis of steady points for systems of differential equations with sigmoid interactions. *Dynamics and Stability of Systems*, 9, 275–291.

Poignard, C., Chaves, M., and Gouzé, J.L. (2016). Periodic Oscillations for Non Monotonic Smooth Negative Feedback Circuits. *SIAM Journal on Applied Dynamical Systems*, 15(1), 257–286.

Ropers, D., de Jong, H., Page, M., Schneider, D., and Geiselmann, J. (2006). Qualitative simulation of the carbon starvation response in *Escherichia coli*. *Biosystems*, 84(2), 124–152.

Shu, Q. and Sanfelice, R.G. (2014). Dynamical properties of a two-gene network with hysteresis. *Information and Computation*, 236, 102–121.

Thomas, R. (1973). Boolean formalization of genetic control circuits. *J. Theor. Biol.*, 42, 563–585.

Thomas, R. and d'Ari, R. (1990). *Biological feedback*. CRC press.

Yagil, G. and Yagil, E. (1971). On the relation between effector concentration and the rate of induced enzyme synthesis. *Biophys. J.*, 11, 1127.